Journal of Biomechanics 60 (2017) 175–180

Contents lists available at ScienceDirect

Journal of Biomechanics

journal homepage: www.elsevier.com/locate/jbiomech
www.JBiomech.com

Model-based cap thickness and peak cap stress prediction for carotid MRI

Annette M. Kok [a,*], Aad van der Lugt [b], Hence J.M. Verhagen [c], Antonius F.W. van der Steen [a], Jolanda J. Wentzel [a], Frank J.H. Gijsen [a]

[a] Department of Biomedical Engineering, Thorax Center, Erasmus Medical Center, Rotterdam, The Netherlands
[b] Department of Radiology, Erasmus Medical Center, Rotterdam, The Netherlands
[c] Department of Vascular Surgery, Erasmus MC, Rotterdam, The Netherlands

ARTICLE INFO

Article history:
Accepted 20 June 2017

Keywords:
Carotid artery
Atherosclerosis
Magnetic resonance imaging
Finite element analysis
Cap thickness
Peak cap stress

ABSTRACT

A rupture-prone carotid plaque can potentially be identified by calculating the peak cap stress (PCS). For these calculations, plaque geometry from MRI is often used. Unfortunately, MRI is hampered by a low resolution, leading to an overestimation of cap thickness and an underestimation of PCS. We developed a model to reconstruct the cap based on plaque geometry to better predict cap thickness and PCS.

We used histological stained plaques from 34 patients. These plaques were segmented and served as the ground truth. Sections of these plaques contained 93 necrotic cores with a cap thickness <0.62 mm which were used to generate a geometry-based model. The histological data was used to simulate in vivo MRI images, which were manually delineated by three experienced MRI readers. Caps below the MRI resolution (n = 31) were (digitally removed and) reconstructed according to the geometry-based model. Cap thickness and PCS were determined for the ground truth, readers, and reconstructed geometries.

Cap thickness was 0.07 mm for the ground truth, 0.23 mm for the readers, and 0.12 mm for the reconstructed geometries. The model predicts cap thickness significantly better than the readers. PCS was 464 kPa for the ground truth, 262 kPa for the readers and 384 kPa for the reconstructed geometries. The model did not predict the PCS significantly better than the readers.

The geometry-based model provided a significant improvement for cap thickness estimation and can potentially help in rupture-risk prediction, solely based on cap thickness. Estimation of PCS estimation did not improve, probably due to the complex shape of the plaques.

1. Introduction

Stroke is the second cause of death worldwide and the third leading cause of disability in the western world (Johnson et al., 2016). One of the causes of an ischemic stroke is atherosclerotic disease in the carotid artery. As a consequence of atherosclerotic plaque rupture, a thrombus might form, which can deprive part of the brain of blood. Several histological studies have provided important insights about plaques that are vulnerable to rupture (Virmani et al., 2002). A vulnerable plaque is characterized by a large and soft lipid rich necrotic core (NC), a thin fibrous cap, and infiltration of macrophages (Falk, 2006).

Plaque rupture occurs when the stresses in the cap exceed the strength of the cap. These cap stresses can be calculated with finite element analysis (FEA). Apart from material properties and boundary conditions, stress computations with FEA critically depend on the geometry of the plaque. Some of the geometry parameters highly influence the cap stresses, including the lumen and the NC curvature, but most importantly the cap thickness (Akyildiz et al., 2015). Geometrical information of carotid plaques is often obtained with magnetic resonance imaging (MRI) because of its ability to distinguish relevant plaque components (Saam et al., 2005). However, the in-plane pixel resolution of a carotid MRI is low. The minimum cap thickness, which is typically around 0.3 mm (Redgrave et al., 2008), is often smaller than the pixel size. Therefore, even experienced MRI readers have difficulties in estimating the minimum cap thickness (CapT); they almost always overestimate the CapT, especially when the caps are thin (H.A. Nieuwstadt et al., 2014a).

* Corresponding author at: Room Ee 2334b, Wytemaweg 80, 3015 CN Rotterdam, The Netherlands.
E-mail address: a.m.kok@erasmusmc.nl (A.M. Kok).

http://dx.doi.org/10.1016/j.jbiomech.2017.06.034
0021-9290/

The overestimation of CapT with MRI will lead to an underestimation of the cap stress. The error in cap stress computations are much higher in the thin caps than in the thick caps (H.A. Nieuwstadt et al., 2014b). A more accurate CapT is needed to improve cap stress calculations.

Previously, we showed that a geometric relation was found between the NC thickness and geometric parameters in coronary arteries (Kok et al., 2016). Here, we apply a similar approach in order to estimate the CapT. We hypothesize that a geometry-based regression model will improve the CapT and thereby also the cap stresses compared to the CapT estimated by the experienced MRI readers.

2. Methods

A graphical summary of the methods is presented in Fig. 1, the steps are explained in detail below.

2.1. Histology

From 34 symptomatic patients (>70% stenosis) who were scheduled for carotid endarterectomy 34 plaques were obtained. All plaques were decalcified and embedded in paraffin and cut in 5 μm sections. The sections were stained with either Elastica van Gieson or Resorcine Fuchsine. In total 76 cross-sections were selected for further analysis, all sections contained at least one NC. The lumen, the NC, and the vessel outer wall were manually delineated. Since these histological plaque cross-sections were not pressure fixated, the contours were computationally pressurized at mean arterial pressure (100 mmHg) with finite element analysis (FEA). These pressurized contours were considered to represent the ground truth geometry.

2.2. Geometry-based model

Since we were interested in the thin caps, all NCs that were located closer than 0.62 mm — a representative value for the clinically used resolution of MRI — to the lumen in the ground truth geometry were selected. Then, the CapT was estimated with a statistical model which was constructed based on geometry features of the plaque. In a previous study, it was shown that lumen area, vessel area and NC area could be quantified accurately with MRI (H.A. Nieuwstadt et al., 2014a). Therefore, in the model the following geometry features were used: (1) the NC angle, (2) the distance from the lumen border to the NC center (Centroid Distance), and (3) the NC thickness, see Fig. 2A. To make the model robust for all plaques sizes, the geometry parameters as well as the output parameter (CapT), were normalized with respect to the corresponding vessel wall thickness, except for the NC angle, which is expressed in radians. To reconstruct the new cap, the model estimated the normalized CapT at three positions. The first position is at the center (50%) of the NC angle and the other two are positioned at the sides (25% and 75%) of the NC angle. One geometry-based model was used for the center and one for the side positions, since these are assumed to be symmetric. The following relation was fitted to the data:

$$CapT_i = \beta_{NC\ angle,i} \times NC\ angle_i + \beta_{Centroid\ Distance,i} \times Centroid\ Distance_i + \beta_{NC\ thickness,i} \times NC\ thickness_i + \beta_{0,i} \quad (1)$$

with β's the parameters as determined with the geometry-based model and i the location at the NC (center or side). All the geometry parameters, NC angle, Centroid Distance and NC thickness, were determined along the line of the corresponding NC angle. The CapT was determined as the minimum cap thickness per segment: in the center (37.5% ≤ NC angle ≤ 62.5%) or at the side positions (NC angle < 37.5 or NC angle > 62.5). The NC area obtained with histology underestimates the NC area obtained via MRI images by 24% (H.A. Nieuwstadt et al., 2014a). To account for this underestimation of the NC area, the NC angle and NC thickness were scaled with $\sqrt{1.24}$. Since a negative CapT is physically not possible and extremely thin caps would lead to extreme and unrealistic stress value. Hence, a cut-off value of 0.069 mm was used for the CapT, which is the mean minimum cap thickness of a fibrous cap minus twice the standard deviation of the minimum cap thickness earlier reported (Cicha et al., 2011).

2.3. MRI segmentation

A subset of 33 cross-sections from 12 patients was used to simulate in vivo carotid MRI images. A clinical MRI protocol was simulated by solving the Bloch equations, with an in-plane resolution for the simulations was 0.62 mm. The protocol was described in more detail by H.A. Nieuwstadt et al. (2014a). Three independent experienced MRI readers manually delineated the lumen, vessel wall, and NCs in the MRI simulated images. In some cases multiple NCs were present in one cross-section. For example, if in a cross-section two NCs were present, the cross-section was analyzed twice; once with one NC and the other NC discarded and vice versa.

2.4. Reconstruction

Reconstruction of the fibrous cap was performed on the cross-sections that met the following criteria: (1) the reader correctly identified the NC, (2) the cap thickness was less than 0.62 mm and, (3) more than 50% of the NC angle of the cap was below 0.62 mm. First, the part of the cap that was thinner than 0.62 mm was removed, see Fig. 2B. The geometry parameters (NC angle, Centroid Distance and NC thickness) obtained by the readers were used to estimate the normalized CapT

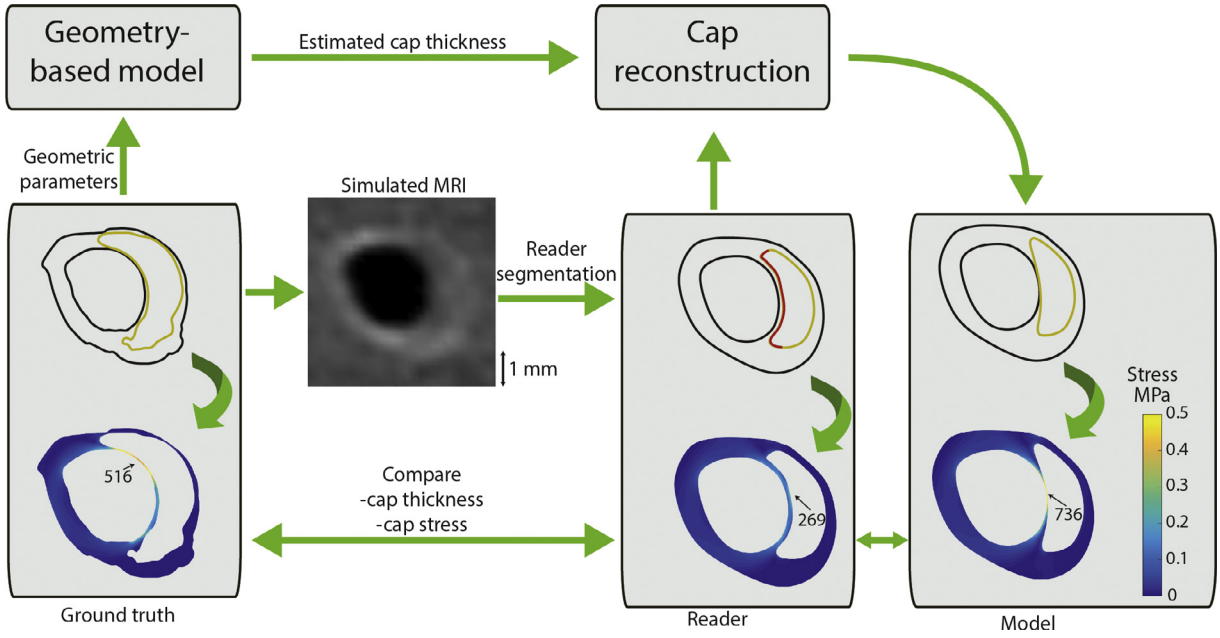

Fig. 1. A schematic overview of the methods section. From the middle left to the middle right: the ground truth (based on histology), reader and model contours with the corresponding stress calculations below. Based on the ground truth contours carotid MRI images were simulated using JEMRIS software. These simulated MRI images were segmented by experienced MRI readers. The cap smaller than 0.62 mm was highlighted in red and was removed for the cap reconstruction. At the right, the cap was reconstructed using cap thickness information from the geometry-based model resulting in new contours ('model') contours.

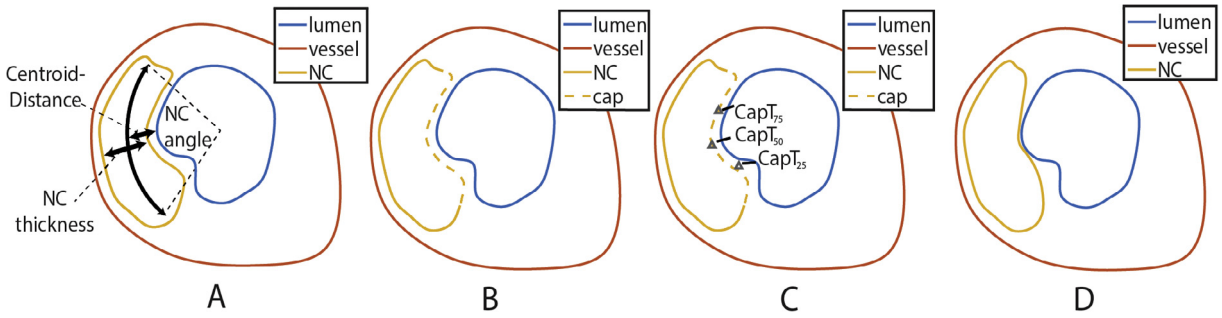

Fig. 2. A schematic overview of the cap reconstruction. (A) the geometry parameters are determined for the geometry-based model visualized for 50% Necrotic core (NC) angle (midcap), this was also done for 25% and 75% NC angle (sidecap), (B) the cap thinner than 0.62 mm was removed, (C) the cap thicknesses estimated by the GEE model are placed at the three locations along the NC angle (D) the remainder of the cap is reconstructed using a Non-Uniform Rational B-Spline (NURBS).

at 25, 50 and 75% of the NC angle. Then, the absolute CapT values were calculated using these normalized CapT by multiplying with the corresponding vessel wall thickness, and placed at that distance from the lumen, see Fig. 2C. Subsequently, a Non-Uniform Rational B-Spline (NURBS) was used to generate the reconstructed cap contour, see Fig. 2D. The reconstruction with the NURBS can cause the CapT to become less than the previous reported cut-off (0.069 mm) value; if this was the case the cap was adjusted using this cut-off value. In order to remove and reconstruct the cap of the NC, MATLAB (version 2014a, Mathworks Inc., Natick, MA, USA) was used.

2.5. Finite element analysis

Wall stress calculations in the plaque geometries were performed with Abaqus (version 6.13, Dassault Systemes Simulia Corp., Providence, RI, USA). Incompressible, Neo-hookean material properties were used for all plaque components (Akyildiz et al., 2011; Badel et al., 2014; Kelly-Arnold et al., 2013). The Young's moduli for the components are 1000 kPa for the intima and 6 kPa for the NC. In order to restrain rigid body movement a soft compressible buffer (Poisson ratio: 0.45, Young's modulus: 60 kPa) was placed around the intima with the outer border fully constraint. Approximately, 100.000 tetrahedral elements were used for the plaque (at least four elements were located across the cap). The initial stresses were calculated at 100 mmHg with the backward incremental method (de Putter et al., 2007; Speelman et al., 2009). The final pressure (125 mmHg) was applied at the lumen contour. Peak cap stress (PCS) was defined as the 99th percentile von Mises stress in front of the cap or in the shoulder region of the cap (15° adjacent to the cap) (Kok et al., 2016).

2.6. Analysis and statistics

For the geometry based model a generalized estimating equations (GEE) method was used, which accounts for using multiple cross sections from one plaque. To quantify the correlation between the ground truth cap thickness and the model cap thickness the r^2 and the concordance correlation coefficient (CCC) were determined. Normal distribution was tested with a Kolmogorov-Smirnov test. Since the data were not normally distributed, the data were reported as median and interquartile range. An ANOVA (with a Bonferroni correction) was used to test absolute differences among groups. The error (with respect to the ground truth) of the cap thickness and PCS observations were paired, and tested with a non-parametric signed Wilcoxon rank test. Especially, the effect of the reconstruction in the thin caps is of interest. Therefore, all data were divided based on the ground truth minimal cap thickness ($CapT_{GT}$), in a thin (<0.1 mm) or a thick (>0.1 mm) cap group. The CapT of the geometry-based model ($CapT_{model}$) and the CapT of the reader ($CapT_{reader}$) were compared with respect to the $CapT_{GT}$. A similar approach was followed for PCS.

3. Results

3.1. Geometry-based model

In total, the 76 cross-sections contained 148 NCs which had the following characteristics: the CapT was 0.23 mm (0.08–0.40 mm), the NC angle was 97.6° (49.7–147°) and the NC thickness at the center of the NC was 0.83 mm (0.39–1.99 mm). Ninety-three NCs had a CapT smaller than 0.62 mm which were used for the construction of the geometry-based regression model. The geometry-based model estimated the normalized CapT, and revealed for both the center and the side positions significant relations, see Table 1. Each of the geometry parameters had a significant ($p < 0.05$) individual effect on the CapT estimation. The parameters showed that the normalized $CapT_{GT}$ was positively related with the normalized Centroid Distance and that it was negatively related with the normalized NC thickness and the NC angle. The geometry-based model for the NC center estimated the normalized $CapT_{model}$ ($r^2 = 0.89$ and $CCC = 0.95$) compared very well to the normalized $CapT_{GT}$, see Fig. 3A. The normalized $CapT_{model}$ for the NC side position was moderately estimated ($r^2 = 0.46$ and $CCC = 0.68$), see Fig. 3B.

3.2. Cap thickness reconstruction

Thirty-one NCs met the reconstruction criteria. The $CapT_{GT}$ was 0.07 mm (0.06–0.11 mm), $CapT_{reader}$ was 0.23 mm (0.18–0.29 mm) and the $CapT_{model}$ was 0.12 mm (0.03–0.22 mm), see Fig. 4A. Fig. 4B shows the absolute $CapT_{GT}$, $CapT_{reader}$, and $CapT_{model}$ for the thin and the thick caps. For the thin cap group, the reader overestimates cap thickness while the $CapT_{model}$ is significantly closer to the ground truth data. For the thick cap group, a similar trend is observed, although not significant. Fig. 4C shows the absolute errors of the $CapT_{model}$ is significantly smaller than those of $CapT_{reader}$ for both thin and thick caps. In 95% of the thin cap cases the CapT estimation improved using the geometry-based model. In contrast, in the thick caps the model improved only 58% of the cases. For the thin caps, the reconstructed geometries predicted the CapT significantly ($p < 0.01$) better than the reader. Also, the reconstructed CapT estimation in the thick caps improved ($p < 0.01$) compared to the reader CapT.

3.3. Wall stress

The PCS_{reader}, 262 kPa (132–356 kPa), almost always underestimated the PCS_{GT}, 464 kPa (311–554 kPa). The PCS_{model}, 384 kPa (228–632 kPa), showed a high variation compared to the PCS_{reader} and the PCS_{GT}, see Fig. 5A. For example the model improved the PCS in NC 16, the reader underestimated the PCS with 161 kPa, and the model made a small overestimation of 58 kPa, with respect to the PCS_{GT}. In contrast, in NC 14 the model does not improve the

Table 1
Generalized Estimation Equation (GEE) parameters with their standard errors. The predictive values, β's, of the GEE model for NC angle, Centroid Distance and the NC thickness and a constant value. NC = Necrotic core.

	$\beta_{NC\,angle}$	$\beta_{Centroid\,Distance}$	$\beta_{NC\,thickness}$	β_0
$CapT_{midcap}$	−0.0278 ± 0.0062	0.82 ± 0.04	−0.35 ± 0.03	0.01 ± 0.02*
$CapT_{\pm sidecap}$	−0.0273 ± 0.01	0.54 ± 0.07	−0.28 ± 0.05	0.12 ± 0.04

* No significant contribution to the model.

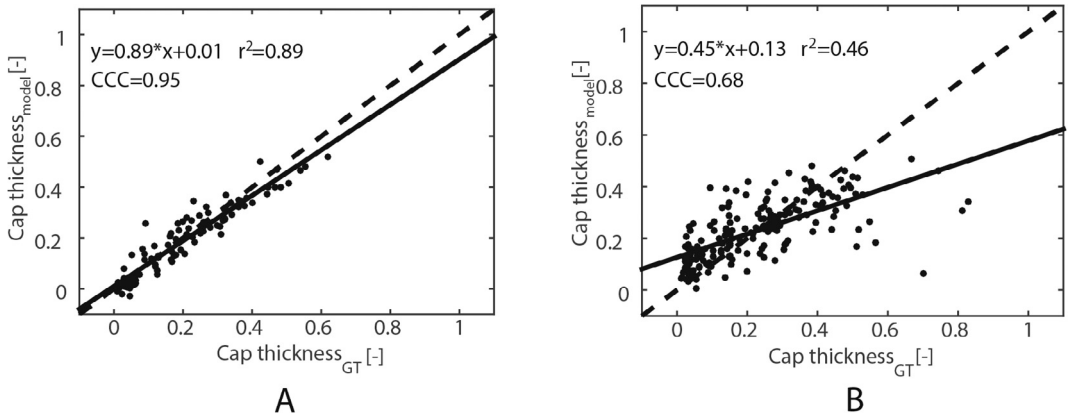

Fig. 3. The normalized estimated cap thickness of the model ($CapT_{model}$) versus the normalized ground truth cap thickness ($CapT_{GT}$) (A) for the midcap and (B) for the sidecap. The dashed line is the line of equality, the solid line is a linear fit through the data.

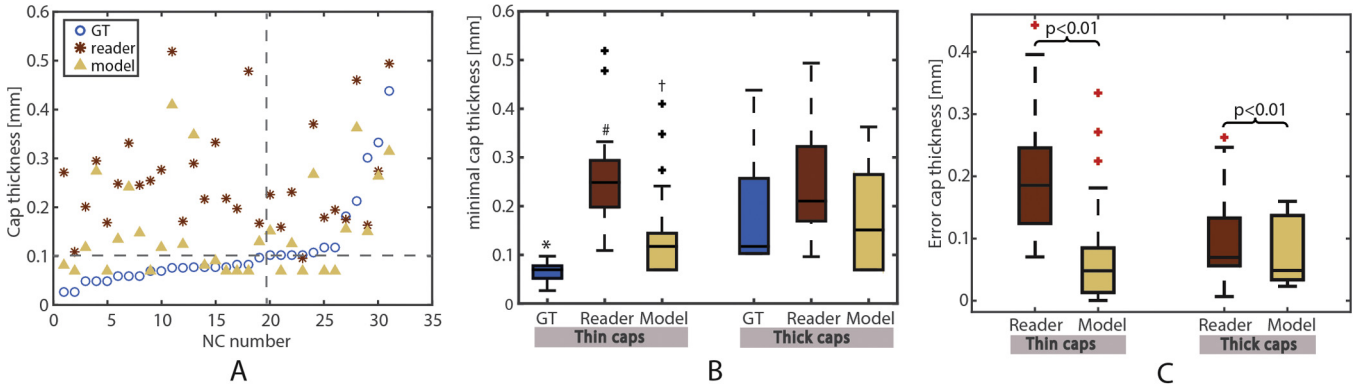

Fig. 4. In (A) the absolute cap thickness values for the ground truth, reader and model geometries. The horizontal grey dotted line indicates 0.1 mm cap thickness, the vertical grey dotted line indicates the division line between thin (<0.1 mm) and thick (>0.1 mm) caps. (B) the absolute cap thickness, on the left the results for the thin caps and on the right for the thick caps. In (C) the absolute cap thickness error with respect to the ground truth, on the left the results for the thin caps and on the right for the thick caps. * = $p < 0.05$ for ground truth vs. reader, # = $p < 0.05$ for ground truth vs. model, ǂ = $p < 0.05$ for reader vs. model.

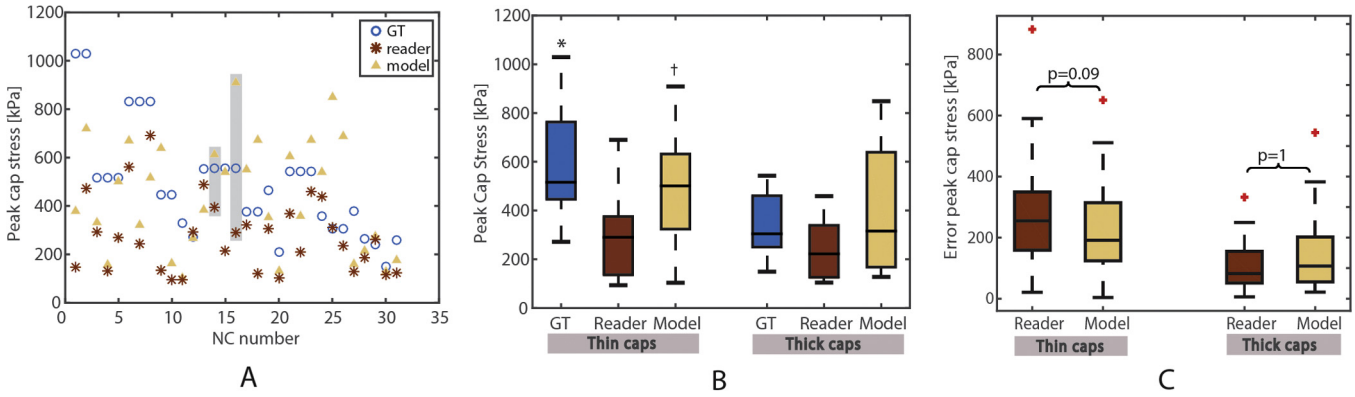

Fig. 5. In (A) the absolute peak cap stress values for the ground truth, reader and model geometries. In grey are the Necrotic Core (NC) numbers 14 and 16 highlighted, which are referred to in the text. In (B) the absolute peak cap stress, on the left the results for thin (<0.1 mm) caps and on the right for the thick (>0.1 mm) caps. In (C) the absolute peak cap stress error with respect to the ground truth cap thickness, on the left the results for thin (<0.1 mm) caps and on the right for the thick (>0.1 mm) caps. * = $p < 0.05$ for ground truth vs. reader, # = $p < 0.05$ for ground truth vs. model, ǂ = $p < 0.05$ for reader vs. model.

PCS, the reader underestimated the PCS by 264 kPa and the model overestimated it by 354 kPa with respect to the PCS_{GT}. There was no significant difference between the PCS_{model} and the PCS_{GT} ($p = 0.21$). Fig. 5B shows the absolute PCS_{GT}, PCS_{reader}, and PCS_{model} for the thin and the thick caps. For the thin caps, the PCS obtained by the reader geometries significantly underestimated the PCS of the ground truth and the model ($p = 0.04$). There was no difference between the PCS_{GT} and the PCS_{model} ($p = 0.24$). For the thick caps a similar trend was observed, however there are no significant differences. Fig. 5C shows that for the thin caps, the absolute stress error of the model geometries was lower than the reader geometries, however not significant ($p = 0.09$). In this group two outliers were observed: one outlier showed an error in PCS_{reader} of 882 kPa and one outlier showed an error of PCS_{model} 651 kPa. These are caused

because the ground truth CapT (0.05 mm) is highly overestimated by the reader (0.30 mm) and model (0.27 mm). For the thick caps, the absolute error in PCS did not improve with the model ($p = 1$). In 74% of the thin cap cases the PCS was improved by the model. In the thick caps, the model improved only 58% of the cases. In the thin caps, the absolute stress error reduced in the reconstructed geometries when comparing to the readers, however this was not significant ($p = 0.09$), see Fig. 5C. In 74% of the thin cap cases the PCS was improved by the model. In the thick caps, the model improved only 58% of the cases. In case of the thin caps, one outlier showed an error in PCS_{reader} of 882 kPa and one outlier showed an error of PCS_{model} 651 kPa. These are caused because the ground truth CapT (0.05 mm) is highly overestimated by the reader (0.30 mm) and model (0.27 mm). For the thick caps, the absolute error in PCS did not improve with the model ($p = 1$).

4. Discussion

For peak cap stress assessment using FEA, a reliable estimate of the cap thickness is essential. MRI readers tend to overestimate the cap thickness and hereby also underestimate the PCS. In this study, we investigated if we can reconstruct the cap with a geometry-based regression model based on geometry features, and thereby improving the estimation of the PCS. The first main finding was that the estimation of the CapT on MR images can be improved using this model. The second main finding was that application of the model, despite the improved CapT estimation, did not lead to a better prediction of PCS.

4.1. Cap thickness

In an earlier study on coronary plaques, we showed an association among NC thickness, NC angle, intima-media thickness and cap thickness (Kok et al., 2016). Therefore, in carotid arteries a relationship between geometry parameters and the normalized CapT was expected. The association between CapT and the geometry features at the NC center was very strong ($r^2 = 0.89$), the model improves the CapT estimation in 81% of the cross-sections. However, the NC side relation was less pronounced, most probably because the fibrous cap was not as symmetric as was assumed.

Shindo et al. found that all carotid plaques with caps above 150 μm were stable (not ruptured) and that all caps lower than 76 μm were ruptured (Shindo et al., 2015). Similar results appeared in a larger histology-based study of symptomatic carotid stenosis patients, which showed that 81% of all plaques lower than 100 μm were ruptured (Redgrave et al., 2008). Therefore, the CapT could be instrumental in indicating the need for surgery. In this study, the sole input to estimate CapT are geometrical plaque features, which can be measured fast and accurately with MRI. Although the model improves CapT estimation in 81% of the cases, in 19% of the cases it does not. In these cases the error of the CapT is in the same range as the CapT associated with carotid rupture prone risk. More research is needed to improve the model before it can be used to predict the rupture risk of an individual plaque. The geometry-based model could also be used to estimate the CapT for plaque de-stabilization studies with respect to medications. For example, statin therapy has already been shown to decrease the NC area and increase CapT (Du et al., 2016; Takarada et al., 2009). If CapT is considered as a secondary endpoint in these studies, this model could be used to better estimate this value.

4.2. Peak cap stress

Peak cap stress is often used as a surrogate marker for rupture risk (Cheng et al., 1993; Tang et al., 2005). In this study we sought a solution for the MRI based overestimation of the CapT, and thereby we hoped to improve the PCS. Interestingly, while in the thin caps the geometry-based model aided in decreasing the CapT error, the PCS showed only a trend towards improvement ($p = 0.09$). Previous studies showed a strong relation between cap thickness and PCS (Akyildiz et al., 2015; Ohayon et al., 2008), but also pointed out the importance of lumen and NC curvature (Akyildiz et al., 2015). Edges of components are smoothed in the MRI model due to the limited spatial resolution which results in a severe underestimation of the curvature. This loss in curvature will lead to an underestimation of the PCS (H.A. Nieuwstadt et al., 2014b). To quantify this loss of detail, we determined the lumen and NC curvature of the ground truth and the reader. We found that the reader curvature was much lower than the ground truth curvature for the lumen: 0.61 mm^{-1} (0.54–0.70 mm^{-1}) vs. 0.98 mm^{-1} (0.78–1.13 mm^{-1}) and for the NC curvature: 0.86 mm^{-1} (0.73–1.02 mm^{-1}) vs. 1.61 mm^{-1} (1.47–2.02 mm^{-1}).

Altogether, it is not recommended to calculate PCS in these thin caps (<0.1 mm) with manually segmented MRI images for rupture risk prediction. Gijsen et al. showed that due to MRI resolution problem, it is better to look for the stable plaque with thick caps and low PCS (Gijsen et al., 2015). We cannot resolve the resolution issue in MRI with a geometry-based model to improve the PCS estimation. Further research is necessary to improve rupture risk assessment based on geometrical plaque features in carotid arteries.

4.3. Limitations

One of the limitations of our study is the relative simple isotropic material model that was used. In diseased tissue, collagen fibers are orientated in a certain direction in order to absorb higher stresses. However, literature on fiber orientation in carotid arteries is sparse. A recent study reported a high dispersion of fibers in carotid arteries (Chai et al., 2014). Therefore, we assume that an isotropic model should be sufficient. Besides, since this is comparison study, we do not expect another material model to change our conclusions.

A relatively low number of caps was reconstructed ($n = 31$) because of several reasons. From the subset of sections that were used for MRI simulation only half of the NCs were identified by the readers. The smaller NCs were probably missed because of the size and the limited resolution. Furthermore, not all NCs that were included had a ground truth cap smaller than 0.62 mm. Although a low number of sections were included in our study, we don't expect that increasing the number would have changed our conclusion on the absence of improvement of PCS because of the large error range of the PCS for the reconstructed NCs.

The geometry-based model to estimate $CapT_{model}$ used all the cross-sections obtained via histology. The same cross-sections were used in the MRI simulations, therefore there might be dependency among the data. As a consequence, our results might be positively influenced. An MR scan prior to endarterectomy combined with histology would be an alternative approach for the MRI simulation. However, in this case 3D registration of the histology with the MR images is needed which is not straight forward, due to several problems including deformation due to histological post-processing, and the limited MRI resolution (Groen et al., 2010), leading to registration errors of 0.6 mm. Thus, 3D registration with histology yields errors larger than the MRI simulations (Groen et al., 2010). Furthermore, Nieuwstadt et al. have shown that the MRI simulation are very similar to in vivo MR images with respect to image contrast, SNR, spatial resolution and intensity gradients over plaque components. Therefore, we chose to simulate the MRI directly from the ground truth histology contours.

5. Conclusion

In conclusion, our model that uses geometry-based features estimates the cap thickness better than experienced MRI readers, which could potentially contribute to risk stratification. The peak cap stress did not significantly improve, probably due to smoothing of other important geometry parameters, such as lumen and NC curvature.

Conflict of interest

None.

Acknowledgements

The research leading to these results has received funding from the European Research Council under the European Union's Seventh Framework Programme / ERC Grant Agreement n. 310457. We would like to thank Jeroen Sonnemans, Gilion Hautvast and Marcel Breeuwer for the MRI segmentations; Kim van Gaalen for the histological processing; and Harm Nieuwstadt for all the fruitful discussions.

References

Akyildiz, A.C., Speelman, L., Nieuwstadt, H.A., van Brummelen, H., Virmani, R., van der Lugt, A., van der Steen, A.F.W., Wentzel, J.J., Gijsen, F.J.H., 2015. The effects of plaque morphology and material properties on peak cap stress in human coronary arteries. Comput. Methods Biomech. Biomed. Engin. 19, 771–779.

Akyildiz, A.C., Speelman, L., van Brummelen, H., Gutiérrez, M.a., Virmani, R., van der Lugt, A., van der Steen, A.F., Wentzel, J.J., Gijsen, F.J., 2011. Effects of intima stiffness and plaque morphology on peak cap stress. Biomed. Eng. Online 10, 25.

Badel, P., Avril, S., Sutton, M.a., Lessner, S.M., 2014. Numerical simulation of arterial dissection during balloon angioplasty of atherosclerotic coronary arteries. J. Biomech. 47, 878–889.

Chai, C.-K., Speelman, L., Oomens, C.W.J., Baaijens, F.P.T., 2014. Compressive mechanical properties of atherosclerotic plaques–indentation test to characterise the local anisotropic behaviour. J. Biomech. 47, 784–792.

Cheng, G.C., Loree, H.M., Kamm, R.D., Fishbein, M.C., Lee, R.T., 1993. Distribution of circumferential stress in ruptured and stable atherosclerotic lesions. A structural analysis with histopathological correlation. Circulation 87, 1179–1187.

Cicha, I., Wörner, A., Urschel, K., Beronov, K., Goppelt-Struebe, M., Verhoeven, E., Daniel, W.G., Garlichs, C.D., 2011. Carotid plaque vulnerability: A positive feedback between hemodynamic and biochemical mechanisms. Stroke 42, 3502–3510.

De Putter, S., Wolters, B.J.B.M., Rutten, M.C.M., Breeuwer, M., Gerritsen, F.A., van de Vosse, F.N., 2007. Patient-specific initial wall stress in abdominal aortic aneurysms with a backward incremental method. J. Biomech. 40, 1081–1090.

Du, R., Zhao, X.-Q., Cai, J., Cui, B., Wu, H.-M., Ye, P., 2016. Changes in carotid plaque tissue composition in subjects who continued and discontinued statin therapy. J. Clin. Lipidol. 10, 587–593.

Falk, E., 2006. Pathogenesis of atherosclerosis. J. Am. Coll. Cardiol. 47. 0–5.

Gijsen, F.J.H., Nieuwstadt, H.a., Wentzel, J.J., Verhagen, H.J.M., van der Lugt, A., van der Steen, A.F.W., 2015. Carotid plaque morphological classification compared with biomechanical cap stress: implications for a magnetic resonance imaging-based assessment. Stroke 46, 2124–2128.

Groen, H.C., van Walsum, T., Rozie, S., Klein, S., van Gaalen, K., Gijsen, F.J.H., Wielopolski, P.A., van Beusekom, H.M.M., de Crom, R., Verhagen, H.J.M., van der Steen, A.F.W., van der Lugt, A., Wentzel, J.J., Niessen, W.J., 2010. Three-dimensional registration of histology of human atherosclerotic carotid plaques to in-vivo imaging. J. Biomech. 43, 2087–2092.

Johnson, W., Onuma, O., Owolabi, M., Sachdev, S., 2016. Stroke: a global response is needed. Bull. World Health Organ. 94. 634–634a.

Kelly-Arnold, A., Maldonado, N., Laudier, D., Aikawa, E., Cardoso, L., Weinbaum, S., 2013. Revised microcalcification hypothesis for fibrous cap rupture in human coronary arteries. Proc. Natl. Acad. Sci. U. S. A. 110, 10741–10746.

Kok, A.M., Speelman, L., Virmani, R., van der Steen, A.F.W., Gijsen, F.J.H., Wentzel, J.J., 2016. Peak cap stress calculations in coronary atherosclerotic plaques with an incomplete necrotic core geometry. Biomed. Eng. Online 15, 48.

Nieuwstadt, H.A., Geraedts, T.R., Truijman, M.T.B., Kooi, M.E., van der Lugt, A., van der Steen, A.F.W., Wentzel, J.J., Breeuwer, M., Gijsen, F.J.H., 2014a. Numerical simulations of carotid MRI quantify the accuracy in measuring atherosclerotic plaque components in vivo. Magn. Reson. Med. 72, 188–201.

Nieuwstadt, H.A., Speelman, L., Breeuwer, M., van der Lugt, A., van der Steen, A.F.W., Wentzel, J.J., Gijsen, F.J.H., 2014b. The influence of inaccuracies in carotid MRI segmentation on atherosclerotic plaque stress computations. J. Biomech. Eng. 136, 021015.

Ohayon, J., Finet, G., Gharib, A.M., Herzka, D.a., Tracqui, P., Heroux, J., Rioufol, G., Kotys, M.S., Elagha, A., Pettigrew, R.I., 2008. Necrotic core thickness and positive arterial remodeling index: emergent biomechanical factors for evaluating the risk of plaque rupture. Am. J. Physiol. Heart Circ. Physiol. 295, H717–H727.

Redgrave, J.N., Gallagher, P., Lovett, J.K., Rothwell, P.M., 2008. Critical cap thickness and rupture in symptomatic carotid plaques: the oxford plaque study. Stroke 39, 1722–1729.

Saam, T., Ferguson, M.S., Yarnykh, V.L., Takaya, N., Xu, D., Polissar, N.L., Hatsukami, T.S., Yuan, C., 2005. Quantitative evaluation of carotid plaque composition by in vivo MRI. Arterioscler. Thromb. Vasc. Biol. 25, 234–239.

Shindo, S., Fujii, K., Shirakawa, M., Uchida, K., Enomoto, Y., Iwama, T., Kawasaki, M., Ando, Y., Yoshimura, S., 2015. Morphologic features of carotid plaque rupture assessed by optical coherence tomography. AJNR Am. J. Neuroradiol. 36, 2140–2146.

Speelman, L., Bosboom, E.M.H., Schurink, G.W.H., Buth, J., Breeuwer, M., Jacobs, M.J., van de Vosse, F.N., 2009. Initial stress and nonlinear material behavior in patient-specific AAA wall stress analysis. J. Biomech. 42, 1713–1719.

Takarada, S., Imanishi, T., Kubo, T., Tanimoto, T., Kitabata, H., Nakamura, N., Tanaka, A., Mizukoshi, M., Akasaka, T., 2009. Effect of statin therapy on coronary fibrous-cap thickness in patients with acute coronary syndrome: Assessment by optical coherence tomography study. Atherosclerosis 202, 491–497.

Tang, D., Yang, C., Zheng, J., Woodard, P.K., Saffitz, J.E., Petruccelli, J.D., Sicard, G.A., Yuan, C., 2005. Local maximal stress hypothesis and computational plaque vulnerability index for atherosclerotic plaque assessment. Ann. Biomed. Eng. 33, 1789–1801.

Virmani, R., Burke, A.P., Farb, A., Kolodgie, F.D., 2002. Pathology of the unstable plaque. Prog. Cardiovasc. Dis. 44, 349–356.